The Origin and Spread of Locally Adaptive Seasonal Camouflage in Snowshoe Hares

Matthew R. Jones,[1,2,*] L. Scott Mills,[3,4] Jeffrey D. Jensen,[2] and Jeffrey M. Good[1,3,*]

1. Division of Biological Sciences, University of Montana, Missoula, Montana 59812; 2. School of Life Sciences, Arizona State University, Tempe, Arizona 85281; 3. Wildlife Biology Program, University of Montana, Missoula, Montana 59812; 4. Office of Research and Creative Scholarship, University of Montana, Missoula, Montana 59812

Submitted November 29, 2019; Accepted March 23, 2020; Electronically published July 20, 2020

Online enhancements: supplemental figures and tables. *Dryad data:* https://doi.org/10.5061/dryad.8gtht76km.

ABSTRACT: Adaptation is central to population persistence in the face of environmental change, yet we seldom precisely understand the origin and spread of adaptive variation in natural populations. Snowshoe hares (*Lepus americanus*) along the Pacific Northwest coast have evolved brown winter camouflage through positive selection on recessive variation at the *Agouti* pigmentation gene introgressed from black-tailed jackrabbits (*Lepus californicus*). Here, we combine new and published whole-genome and exome sequences with targeted genotyping of *Agouti* to investigate the evolutionary history of local seasonal camouflage adaptation in the Pacific Northwest. We find evidence of significantly elevated inbreeding and mutational load in coastal winter-brown hares, consistent with a recent range expansion into temperate coastal environments that incurred indirect fitness costs. The genome-wide distribution of introgression tract lengths supports a pulse of hybridization near the end of the last glacial maximum, which may have facilitated range expansion via introgression of winter-brown camouflage variation. However, signatures of a selective sweep at *Agouti* indicate a much more recent spread of winter-brown camouflage. Through simulations, we show that the delay between the hybrid origin and subsequent selective sweep of the recessive winter-brown allele can be largely attributed to the limits of natural selection imposed by simple allelic dominance. We argue that while hybridization during periods of environmental change may provide a critical reservoir of adaptive variation at range edges, the probability and pace of local adaptation will strongly depend on population demography and the genetic architecture of introgressed variation.

Keywords: adaptive introgression, climate change, genetic load, genomics, range expansion.

* Corresponding authors; email: jonesmr9@gmail.com, jeffrey.good@umontana.edu.

ORCIDs: Jones, https://orcid.org/0000-0002-4822-157X; Mills, https://orcid.org/0000-0001-8771-509X; Jensen, https://orcid.org/0000-0002-4786-8064; Good, https://orcid.org/0000-0003-0707-5374.

Am. Nat. 2020. Vol. 196, pp. 000–000.
DOI: 10.1086/710022

Introduction

Local adaptation is fundamental to the persistence of populations during periods of rapid environmental change. In particular, local adaption to marginal habitats may increase a species' niche breadth and range size (Holt and Gomulkiewicz 1997), enhancing their evolutionary resilience (Sgrò et al. 2011; Slatyer et al. 2013; Forsman 2016; Mills et al. 2018). Consequently, range edges where populations encounter marginal habitats and less favorable conditions may harbor crucial adaptive variation that facilitates long-term persistence in the face of environmental change (Hampe and Petit 2005; Hill et al. 2011; Cheng et al. 2014). Yet range boundaries may also reflect the limits of natural selection if they are defined by environments where populations have failed to adapt (Antonovics 1976; Kirkpatrick and Barton 1997; Bridle and Vines 2007). Revealing how adaptive variation arises and spreads along range edges is therefore fundamental to understanding the limitations of adaptation to new or changing environments (Ackerly 2003; Hampe and Petit 2005). However, we rarely possess detailed knowledge of the genetic basis and evolutionary history of local adaptation in natural populations.

Several decades of theoretical research have established a framework for predicting demographic conditions along range margins, which are crucial in shaping population-level fitness and the potential for adaptation and range expansion. Populations inhabiting marginal habitats are generally predicted to be small and occur at low densities (Antonovics 1976; Kirkpatrick and Barton 1997), resulting in relatively reduced rates of beneficial mutation and levels of standing genetic variation (Pfennig et al. 2016). Small range-edge populations may further experience higher rates of inbreeding due to genetic drift (Wright 1931; Barton 2001) and accumulate deleterious variation (i.e., mutational load; Lynch et al. 1995; Willi et al. 2018), which can decrease the probability of population persistence (Mills and Smouse 1994).

Elevated individual inbreeding and mutational load along range edges may also reflect past histories of adaptation and range expansion that result in nonequilibrium population dynamics. For instance, mating between close relatives may increase in founder populations that have recently undergone severe population contractions associated with range expansions (Frankham 1998). Likewise, mutational load may be amplified through the colonization of new environments because population contractions reduce the efficacy of selection against deleterious alleles at the expansion front (i.e., expansion load; Peischl et al. 2013; Henn et al. 2016; González-Martínez et al. 2017; Willi et al. 2018). When adaptation does occur along range margins, it may therefore produce negative feedbacks on population fitness and evolutionary potential.

Patterns of migration into range-edge populations are also pivotal to their fitness and adaptive potential. Larger core populations are expected to produce relatively more migrants than smaller edge populations, leading to asymmetric rates of gene flow between core and peripheral habitats. In extreme scenarios, edge populations with low population growth rates ($\lambda < 1$) can be demographic sinks that are maintained by immigration from the core of the range (Holt and Gomulkiewicz 1997; Griffin and Mills 2009). Highly asymmetric gene flow may further reduce fitness and hinder adaptation along the range edge by continually swamping local selection (Haldane 1930; Garcia-Ramos and Kirkpatrick 1997; Kirkpatrick and Barton 1997; Kawecki 2008). However, gene flow from core populations into edge populations may ultimately promote adaptive responses when edge populations are small and ecological gradients are shallow (Polechová 2018; Bontrager and Angert 2019).

Hybridization between species may also facilitate adaptation and range expansion if edge populations intersect with the range of closely related species that are adapted to local habitats (Baker 1948; Lewontin and Birch 1966; Burke and Arnold 2001; Rieseberg et al. 2007; Kawecki 2008; Pfennig et al. 2016). Introgression may provide a crucial source of large-effect variation (Hedrick 2013), which is predicted to be scarce in small populations but often necessary for range-edge adaptation and expansion (Behrman and Kirkpatrick 2011; Gilbert and Whitlock 2016). Putative adaptive introgression has now been shown in numerous species (e.g., Song et al. 2011; Pardo-Diaz et al. 2012; Huerta-Sánchez et al. 2014; Lamichhaney et al. 2015; Miao et al. 2016; Jones et al. 2018; Oziolor et al. 2019) and has been specifically linked to range expansions in Australian fruit flies (Lewontin and Birch 1966), sunflowers (Rieseberg et al. 2007), and mosquitoes (Besansky et al. 2003). While hybridization may facilitate adaptation and range expansion via large-effect mutations (Hedrick 2013; Nelson et al. 2019), the factors influencing the pace of adaptive introgression are often unclear.

Snowshoe hares (*Lepus americanus*) are broadly distributed across boreal and montane forests of North America. Most populations of hares undergo seasonal molts between brown (summer) and white (winter) coats to maintain crypsis in snow-covered environments. Seasonal camouflage is a crucial component of fitness in this system (Mills et al. 2013), as hares that become mismatched with their environment experience dramatically increased predation rates (i.e., 3%–7% increase in weekly mortality; Zimova et al. 2016). However, some hares have adapted to mild winter environments by remaining brown in the winter (Mills et al. 2018). Brown winter camouflage in snowshoe hares is relatively rare across the entire range (<5% of the range) but is predominant along portions of the southern range edge in the Pacific Northwest (Nagorsen 1983), with occurrence closely tracking regions of low seasonal snow cover (Mills et al. 2018). As snow cover across North America continues to decline under climate change, it is predicted that winter-brown camouflage may spread from the edge to the interior of the range, enhancing the evolutionary resilience of snowshoe hares (Jones et al. 2018, 2020; Mills et al. 2018). We previously demonstrated that brown versus white winter camouflage in Pacific Northwest snowshoe hares is determined by a *cis*-regulatory polymorphism at the *Agouti* pigmentation gene that influences its expression during the autumn molt (Jones et al. 2018). The winter-brown allele is fully recessive and derived from introgressive hybridization with black-tailed jackrabbits (*Lepus californicus*), a closely related scrub-grassland species that remains brown in the winter (Jones et al. 2018). Furthermore, the winter-brown haplotype shows signatures of a hard selective sweep in Pacific Northwest localities from Oregon, Washington, and southern British Columbia, consistent with strong selection for local camouflage adaptation (Jones et al. 2018). Thus, the evolution of brown winter coats along coastal environments in the Pacific Northwest represents one of the few verified cases of introgression underlying an adaptive trait of known ecological relevance in mammals (Taylor and Larson 2019).

The establishment of this genotype-to-phenotype link provides a powerful opportunity to examine how population history and hybridization shape local adaptation and expansion along the range edge. Here, we seek to deepen our understanding of (1) the population history of Pacific Northwest range-edge snowshoe hares and (2) the origin and spread of winter-brown camouflage across coastal Pacific Northwest environments. We first use previously published targeted exome data (61.7 Mb for 80 individuals; Jones et al. 2018) to estimate historical changes in population size, individual inbreeding coefficients, and mutational load in Pacific Northwest hares. We then combine whole-genome sequences (WGS; six new and five previously published) with 61 newly assembled complete mitochondrial

genomes and targeted genotyping of the introgressed *Agouti* region across 106 hares to resolve the timing of hybridization with black-tailed jackrabbits and the subsequent spread of winter-brown coat color variation. We use these data to test theoretical predictions for the maintenance and spread of adaptive variation in peripheral environments. Our study provides rare empirical insight into the dynamic interplay of environmental change, hybridization, and selection along range-edge environments and its evolutionary consequences.

Methods

Genomic Data Generation

All sample collection with live animals was performed under approved state permits and associated animal use protocols approved through the University of Montana Institutional Animal Care and Use Committee.

For some analyses, we used previously generated targeted whole-exome data (61.7 Mb spanning 213,164 intervals, ~25-Mb protein-coding exons, an ~28-Mb untranslated region, and ~9-Mb intronic or intergenic regions) for 80 snowshoe hares (21× mean coverage per individual) collected from Washington (winter brown, $n = 13$; winter white, $n = 13$), Oregon (winter brown, $n = 13$; winter white, $n = 13$), Montana (winter white, $n = 14$), and southwest British Columbia (winter brown, $n = 14$; Jones et al. 2018). Hares from Oregon and Washington were collected in the Cascade Range, where populations are polymorphic for winter coat color (fig. 1*A*). Hares from Seeley Lake in western Montana are winter-white individuals, while those from British Columbia were collected in low-lying regions near the Pacific coast, where snowshoe hares are all winter brown (fig. 1*A*). To infer the history of hybridization, we performed whole-genome resequencing of three black-tailed jackrabbits from Oregon and California and two winter-brown snowshoe hares from Oregon and British Columbia. These samples complement WGS data previously generated for two black-tailed jackrabbits from Nevada (one of which was sequenced to higher coverage in this study) and snowshoe hares from Montana, Washington, Utah, and Pennsylvania (Jones et al. 2018). We extracted genomic DNA following the Qiagen DNeasy Blood and Tissue kit protocol and prepared genomic libraries following the KAPA Hyper prep kit manufacturer's protocol. For all libraries, we sheared genomic DNA using a Covaris E220evolution ultrasonicator and performed a stringent size selection using a custom-prepared carboxyl-coated magnetic bead mix (Rohland and Reich 2012) to obtain average genomic fragment sizes of 400–500 bp. We determined indexing polymerase chain reaction (PCR) cycle number for each library with quantitative PCR (qPCR) on a Stratagene Mx3000P thermocycler (Applied Biosystems) using a DyNAmo Flash SYBR Green qPCR kit (Thermo Fisher Scientific). Final libraries were size selected again with carboxyl-coated magnetic beads, quantified with a Qubit (Thermo Fisher Scientific), and pooled for sequencing by Novogene on two lanes of Illumina HiSeq4000 using paired-end 150-bp reads.

To resolve the history of selection on the winter-brown *Agouti* allele, we performed targeted enrichment and sequencing to genotype 106 hares at the *Agouti* locus (Washington, $n = 37$; Oregon, $n = 64$; Montana, $n = 5$). We developed a custom set of IDT xGen Lockdown probes spanning a 596.4-kb interval centered on the *Agouti* gene and extending to flanking regions (chr4:5250800–5847200; coordinates are based on the European rabbit [*Oryctolagus cuniculus*] oryCun2 genome build). The probe sequences were based on a snowshoe hare pseudoreference genome (~33× mean coverage; Jones et al. 2018) derived from iterative mapping to the rabbit genome (Carneiro et al. 2014). We targeted 96 uniquely mapped 100-bp regions (based on low-coverage WGS data from Jones et al. 2018) that contained one or more diagnostic single-nucleotide polymorphisms (SNPs) for winter coat color, allowing us to infer winter coat color for samples based on their *Agouti* genotype. We prepared genomic libraries for targeted *Agouti* sequencing following a modified version of Meyer and Kircher (2010), as described in Jones et al. (2018). We performed hybridization reactions on 500 ng of pooled libraries (10–16 individual libraries per pool), 5 μg of custom-prepared snowshoe hare C_0t-1 DNA, and 2 nM blocking oligos. Washing and recovery of captured DNA was performed following the IDT xGen Lockdown probe hybridization capture protocol (ver. 2). Each capture library was then amplified in 50-μL reactions with 1× Herculase II reaction buffer, 250 μM each dNTP, 0.5 μM each primer, 1 μL of Herculase II fusion polymerase, and 20 μL of library template. The PCR temperature profile consisted of a 45-s 98°C denaturation step followed by 24 cycles of 98°C for 15 s, 60°C for 30 s, and 72°C for 30 s, with a final 72°C elongation step for 1 min. We cleaned and size selected final libraries with 1.2× carboxyl-coated magnetic beads and verified target enrichment with qPCR. *Agouti* capture libraries were then pooled and sequenced with other libraries across two lanes of Illumina HiSeq4000 at the University of Oregon Core (Eugene, OR) and Novogene.

Read Processing and Variant Calling

For all raw sequence data, we trimmed adapters and low-quality bases (mean phred-scaled quality score <15 across a 4-bp window) and removed reads shorter than 50 bp using Trimmomatic (ver. 0.35; Bolger et al. 2014). We then merged paired-end reads overlapping more than 10 bp and with less than 10% mismatched bases using FLASH2

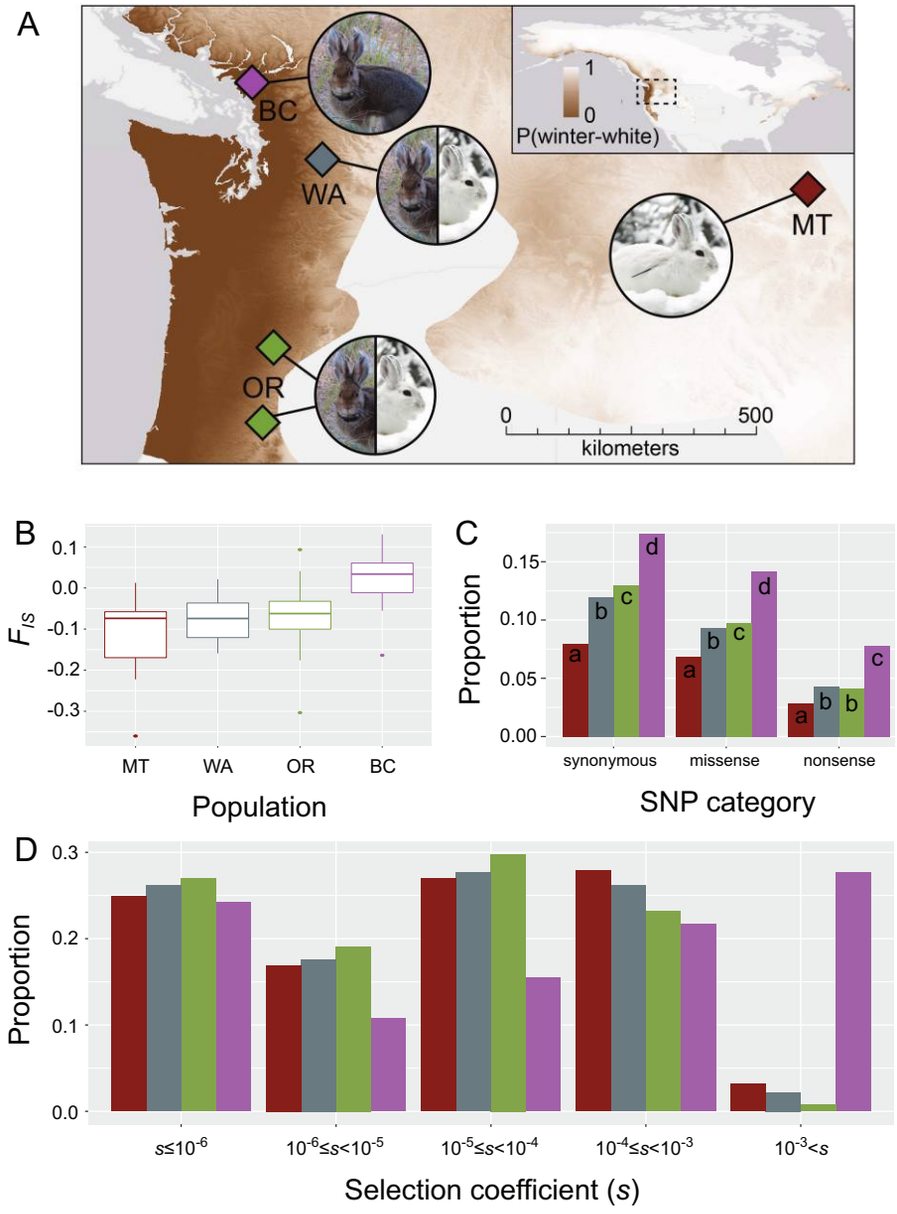

Figure 1: *A*, Snowshoe hare range map colored by the probability of winter-white camouflage (underlying model from Mills et al. 2018). The Pacific Northwest region is magnified and shows sampling localities and coat color phenotypes for British Columbia (BC; purple), Montana (MT; red), Oregon (OR; green), and Washington (WA; blue) populations used to generate whole-exome data. *B*, Box-and-whisker plots representing distributions of individual inbreeding coefficients (F_{IS}) within each population. *C*, Proportion of homozygosity across Pacific Northwest populations for single-nucleotide polymorphisms (SNPs) classified as synonymous, missense, or nonsense. Different letters under each SNP category denote significant differences between populations ($P < .01$; e.g., b is significantly higher than a and lower than c). *D*, Inferred distribution of fitness effects for each population shown as the proportion of mutations with given selection coefficients.

(Magoč and Salzberg 2011). Cleaned exome and *Agouti* capture reads were mapped using default settings in BWA-MEM (ver. 0.7.12; Li 2013) to the snowshoe hare pseudoreference genome. WGS data were mapped to either the snowshoe hare or a black-tailed jackrabbit pseudoreference, which was also created by iteratively mapping to the rabbit genome (Jones et al. 2018). We used PicardTools to remove duplicate reads with the MarkDuplicates function and assigned read group information with the AddOrReplaceReadGroups function. Using GATK (ver. 3.4.046; McKenna et al.

2010), we identified poorly aligned genomic regions with RealignerTargetCreator and performed local realignments with IndelRealigner. We performed population-level multisample variant calling using default settings with the GATK UnifiedGenotyper and filtered variants in VCFtools (ver. 0.1.14; Danecek et al. 2011). For whole-exome and whole-genome data, we filtered genotypes with individual coverage <5× or >70× or with a phred-scaled quality score <30. Additionally, we removed all indel variants and filtered SNPs with a phred-scaled quality score <30 and Hardy-Weinberg $P < .001$. We required that sites have no missing data across individuals. For targeted *Agouti* SNP data, we additionally filtered heterozygous genotypes with allelic depth ratios >3 and sites with >50% missing data across individuals. We phased haplotypes and imputed missing data with Beagle (ver. 4.1; Browning and Browning 2007) and used Haplostrips (Marnetto and Huerta-Sánchez 2017) to visualize haplotype structure.

Population Size History and Inbreeding Coefficients of Pacific Northwest Hares

We used the program ∂a∂i (Gutenkunst et al. 2009) to infer historical population size (N) changes in Pacific Northwest snowshoe hare populations (British Columbia, Montana, Oregon, and Washington) using the folded site frequency spectrum (SFS) of synonymous variants from our whole-exome data set. We used the folded SFS to be consistent with statistical inferences of the distribution of fitness effects (see below). For each population, we tested a standard neutral equilibrium model, a two-epoch model (single instantaneous N change), a three-epoch model (two instantaneous N changes), an exponential N growth model, and an instantaneous N change plus exponential N growth model. We inferred values for parameters ν, representing the population size relative to ancestral N (N_{anc}; e.g., $\nu = 10$ if $N = 10 \times N_{anc}$), and t, representing the time of population size changes in units of $2N_{anc}$ generations. We performed 100 independent runs under each model starting with parameter values sampled randomly across a uniform distribution ($0.001 < \nu < 100$, $0 < 2N_e t < 2$). For each model, we selected parameters with the highest log-likelihood value and chose the overall best model using a composite-likelihood ratio test with the Godambe information matrix (Coffman et al. 2016). We further checked the validity of maximum likelihood models by comparing the predicted SFS to the observed SFS for each population (fig. S2; figs. S1–S4 are available online). We determined 95% confidence intervals (CIs) for parameter estimates using the Godambe information matrix with 100 bootstrap data sets composed of one randomly selected synonymous SNP per 10 kb.

SFS-based approaches are often underpowered or inappropriate for inferring recent population size changes (Robinson et al. 2014; Beichman et al. 2018). For instance, even with a sufficient sample size, a historically large population that has very recently contracted in size (i.e., not in equilibrium) may nonetheless have a large variance N_e. However, individuals in such populations may exhibit elevated individual inbreeding coefficients (F_{IS}), calculated as $1 - H_o/H_e$, where H_o is the observed heterozygosity and H_e is expected heterozygosity assuming random mating. To examine evidence for recent population contractions, we calculated the mean F_{IS} for each population using VCFtools (–het) and tested for significant differences between populations with a two-tailed Student's t-test in R (t.test in the stats package; R Core Team 2018).

Mutational Load and the Distribution of Fitness Effects

For each Pacific Northwest population, we measured the proportion of homozygosity across SNPs with predicted phenotypic effects (missense and nonsense nonsynonymous mutations) as an indicator for relative differences in mutational load under a recessive deleterious mutation model (González-Martínez et al. 2017). We tested for significant differences in the proportion of homozygosity across populations using two-sided Z-tests for proportions in R (prop.test in the stats package; R Core Team 2018). Additionally, we used whole-exome data to infer the distribution of selection coefficients of segregating variation, commonly referred to as the distribution of fitness effects (DFE). In principle, we can infer the DFE from the SFS of sites under selection because neutral, weakly deleterious, and strongly deleterious variation should segregate at different frequencies in populations (Keightley and Eyre-Walker 2010). The DFE of segregating variation is commonly inferred by first fitting a population history model to the SFS of neutral sites (often synonymous SNPs) and then fitting a mutational model to the SFS of selected sites (often nonsynonymous SNPs) while controlling for the effects of population history on the SFS of selected sites (Keightley and Eyre-Walker 2010). Here, we implemented this approach using the Fit∂a∂i module (Kim et al. 2017). We used the maximum likelihood parameter values from our inferred demographic model to control for population history and fit a simple DFE to the folded SFS of nonsynonymous variants (identified with SNPeff; Cingolani et al. 2012) described by a gamma distribution of selective effects with a shape (α) and scale (β) parameter. To estimate variance in α and β, we used 100 bootstrap data sets randomly sampling 50% of nonsynonymous sites and performed 10 independent runs on each data set. We used random starting values between 0.001 and 1 for α and values between 0.01 and 200,000 for β. To scale the DFE from relative selection coefficients ($2N_{anc}s$) to absolute selection coefficients (s), we divided β by $2N_{anc}$ (Kim et al. 2017).

The Timing of Hybridization

If hybridization between snowshoe hares and black-tailed jackrabbits is rare, then the age of hybridization may also reflect the age of *Agouti* introgression. We used two complementary approaches to estimate the timing of hybridization between Pacific Northwest snowshoe hares and black-tailed jackrabbits. Previous phylogenetic analysis of partial cytochrome *b* sequences revealed that some Pacific Northwest snowshoe hares carry introgressed mitochondrial DNA (mtDNA) genomes derived from hybridization with black-tailed jackrabbits (Cheng et al. 2014; Melo-Ferreira et al. 2014). We estimated the age of mtDNA introgression using complete mtDNA genomes for snowshoe hares ($n = 56$) and black-tailed jackrabbits ($n = 5$) that we assembled de novo from newly and previously generated WGS data (Jones et al. 2018) with the program NOVOPlasty (Dierckxsens et al. 2017). We aligned individual mtDNA assemblies, including the rabbit mtDNA reference as an out-group (total assembled length: 16,251 bp), using default settings in Clustal W (ver. 2.1; Larkin et al. 2007) and visually verified alignment quality. We then estimated a maximum clade credibility tree and node ages with a calibrated Yule model in BEAST 2 (Bouckaert et al. 2014), assuming a strict molecular clock and an Hasegawa-Kishono-Yano (HKY) substitution model using empirical base frequencies. We specified default priors for the kappa and gamma shape parameters and used a gamma distribution ($\alpha = 0.001, \beta = 1{,}000$) as a prior for the clock rate and birth rate parameter. We ran the Markov chain Monte Carlo (MCMC) for 5 million steps and calibrated divergence times using a lognormal distribution for the rabbit-*Lepus* node age with a median of 11.8 million generations (95% prior density: 9.8–14.3; Matthee et al. 2004).

We also examined patterns of autosomal introgression tracts to infer the age of nuclear admixture. Given that mtDNA admixture may have been relatively ancient (Melo-Ferreira et al. 2014), admixture dating approaches based on linkage disequilibrium (LD) may have low power because of erosion of LD through ongoing recombination (Loh et al. 2013). Therefore, we developed an approach to fit the distribution of empirically inferred introgression tract lengths to tract lengths simulated under various models of admixture. We first identified genome-wide tracts of introgression using the program PhyloNet-HMM (Liu et al. 2014), which assigns one of two parent trees (species tree or hybridization tree) to each variable position using a hidden Markov model. PhyloNet-HMM robustly distinguishes between incomplete lineage sorting (ILS) and introgression by allowing for switches between gene trees within each parent tree (Liu et al. 2014; Schumer et al. 2016). Alignments of WGS data for the phylogenetic analysis included two black-tailed jackrabbits sampled from California (BTJR1) and Nevada (BTJR2), a Utah snowshoe hare (previously shown as nonadmixed; Jones et al. 2018), and a winter-brown Washington snowshoe hare to represent the admixed Pacific Northwest snowshoe hare population. Here, the species tree is defined as ((Washington, Utah), (BTJR1, BTJR2)), and the hybridization tree is defined as (Utah, (Washington, BTJR1/BTJR2)). We specified base frequencies and transmission/transversion rates on the basis of analysis with RAxML (ver. 8.2.8; Stamatakis 2014). We identified introgression tracts as contiguous regions of the genome with an average hybridization tree probability >95% across 25 variant windows (one variant step) and excluded introgression tracts shorter than 10 kb (Schumer et al. 2016). We then used the program SELAM (Corbett-Detig and Jones 2016) to simulate introgression tract length distributions under various admixture scenarios. We simulated a single pulse of admixture lasting either one generation or 100 generations and occurring at a frequency of 0.01%, 0.1%, or 1%. We recorded introgression tracts >10 kb every 1,000 generations for 50,000 generations across 21 autosomes. We also simulated two pulses of admixture (at a rate of 0.01% and each lasting a single generation) spaced 10,000 generations apart and a low rate of continuous admixture (0.001%). We performed a goodness-of-fit test between the empirical tract length distribution and simulated tract length distributions through time using Kolmogorov-Smirnov tests, which measure differences in the cumulative fraction of data across the range of observed values (Massey 1951). Here, the model fit is measured with the *D* statistic, which varies from 0 (a perfect fit) to 1. To estimate the variance in hybridization timing, we performed Kolmogorov-Smirnov tests in R (ks.test in the stats package; R Core Team 2018) on 100 bootstrap data sets generated by subsampling 30% of the empirical genome-wide introgression tracts.

The Time to Most Recent Common Ancestor of the Winter-Brown Haplotype

To understand the history of the spread of brown winter camouflage, we used targeted *Agouti* SNPs to estimate the time to the most recent common ancestor (TMRCA) for the winter-brown *Agouti* haplotype in Oregon ($n = 47$ individuals) and Washington ($n = 35$ individuals). British Columbia individuals were excluded from this analysis because of limited individual sampling and low genomic coverage. We estimated the TMRCA using a MCMC approach implemented in startmrca (Smith et al. 2018), which leverages information on the length distribution of the fixed selected haplotype and the accumulation of derived mutations. We assumed a constant recombination rate of 1 cM/Mb (Carneiro et al. 2011) and tested an upper and lower estimate for mutation rate based on the European rabbit (2.02×10^{-9} and 2.035×10^{-9} mutations/site/generation;

Carneiro et al. 2012). We also explored the influence of using a divergent population (five homozygous winter-white individuals from Montana) or a local population (19 homozygous winter-white individuals from Oregon and Washington) to represent the ancestral winter-white haplotype (Smith et al. 2018). We assumed chr4:5480355 (in oryCun2 coordinates) as the site of the "selected allele," which lies in the center of the association interval between two strong candidate insertion-deletion mutations in the 5′ *cis*-regulatory region of *Agouti* and is perfectly correlated with winter coat color (Jones et al. 2018). We performed 100,000 iterations with a standard deviation of 20 for the proposal distribution and used the final 10,000 iterations to generate posterior TMRCA distributions (Smith et al. 2018).

Simulations of Selection on a Recessive Beneficial Allele

Assuming fixation of a single haplotype, the above framework for inferring the TMRCA should reflect the age at which the beneficial haplotype began to increase rapidly in frequency (Smith et al. 2018), which under some conditions may be much more recent than the age at which the beneficial mutation entered the population (Teshima and Przeworski 2006; Kelley 2012). For instance, the masking of recessive alleles to selection at low frequency is expected to decrease the rate at which they begin to increase in frequency, conditional on fixation (Teshima and Przeworski 2006), potentially resulting in a temporal lag between a fixed allele's origin and the TMRCA from startmrca (Smith et al. 2018). However, such a scenario may be unlikely, as the masking of rare recessive alleles is also expected to decrease their fixation probability (i.e., Haldane's sieve; Haldane 1924; Turner 1981). Alternatively, an environmental change could favor a previously neutral or deleterious variant, resulting in a delayed spread of a segregating mutation. Indeed, Orr and Betancourt (2001) demonstrated that the bias against fixation of recessive alleles disappears when positive selection acts on preexisting variation in mutation-selection balance. We used simulations to test whether different estimates of the timing of hybridization (i.e., the origin of the winter-brown haplotype) and TMRCA of the winter-brown allele could be due to the masking of recessive alleles at low frequency. Using SLiM (ver. 3.1; Haller and Messer 2019), we simulated an equilibrium population ($N_e = 257{,}219$ for the Oregon population; table 1) experiencing positive selection on a recessive allele ($s = 0.026$, which reflects our updated median estimate of s for winter-brown haplotype in Oregon; Jones et al. 2018). At the beginning of the simulations, the recessive allele was introduced at a rate of 0.01% or 0.1% per generation for 1 or 100 generations, which reflects various rates and durations of hybridization. Under each hybridization scenario, we performed 100 simulations and tracked the frequency of the recessive allele every generation, conditioning on fixation. We saved tree sequences (Haller et al. 2019) and analyzed them using msprime (Kelleher et al. 2016) to identify the TMRCA for fixed beneficial alleles and determine whether selection resulted in fixation of a single copy (hard sweep) or multiple copies (soft sweep) of the beneficial allele.

Results

Range-Edge Population History and Mutational Load

We found support for a single relatively strong N contraction (i.e., a two-epoch model) occurring ~24–100 thousand generations ago (kga) in Oregon, Washington, and British Columbia hares (table 1; fig. S2). In contrast, the history of the Montana population was characterized by an instantaneous plus exponential N change model, in which the population experienced a sudden 17× expansion ~129 kga

Table 1: Maximum likelihood demographic model parameter estimates

Population	Model	N_{anc}	N_B	N_F	t
Montana	Instantaneous change plus exponential growth	459,809 (450,035–469,582)	8,121,810 (5,984,297–10,344,665)	245,430 (197,252–295,473)	129,400 (98,087–161,953)
British Columbia	Two epoch	669,265 (662,769–675,760)	210,484 (184,353–237,086)	...	97,853 (70,702–125,517)
Washington	Two epoch	509,979 (503,464–516,493)	161,654 (125,444–198,747)	...	24,357 (20,061–28,755)
Oregon	Two epoch	494,903 (482,587–507,220)	257,219 (191,394–326,076)	...	52,540 (44,017–61,431)

Note: Values in parentheses are 95% confidence intervals. N_{anc} = population size of common ancestor; N_B = population size following instantaneous change at time t (in generations); N_F = population size following an exponential change beginning immediately after time t.

followed by a gradual reduction to ~53% of N_{anc}. Despite population contractions, estimates of contemporary N_e across all populations were relatively large (161,654–257,219; table 1). Data underlying these models have been deposited in the Dryad Digital Repository (https://doi.org/10.5061/dryad.8gtht76km; Jones 2020).

Using the same exome data set, we previously estimated the joint SFS for pairs of snowshoe hare populations to infer histories of population split times, migration rates, and effective population size in ∂a∂i (Jones et al. 2018). These pairwise models supported histories of high symmetrical migration rates between populations and N contractions following population splits but generated significantly smaller estimates of contemporary N_e compared with the new estimates that we report in table 1. However, we made a scaling error while estimating θ ($=4N_e\mu$) under these previous models. This error affected our previously reported demographic parameter estimates for snowshoe hares (table S9 in Jones et al. 2018) and associated selection coefficient parameter estimates (e.g., previous mean: $s = 0.024$ for Washington, $s = 0.015$ for Oregon; updated mean: $s = 0.049$ for Washington, $s = 0.027$ for Oregon) but not the main inference of introgression at *Agouti* underlying the genetic basis of polymorphic coat color in snowshoe hares. After scaling parameter values to the correct value of θ and excluding models beyond a priori divergence time parameter bounds (>500 kga), we found that our maximum likelihood demographic model (reported here in table S1; tables S1–S3 are available online) still includes high migration rates between populations (~1–2.63 migrants/generation), but with N_e estimates that are appreciably larger than we previously reported and that are comparable to our new estimates (table 1).

We found significantly elevated F_{IS} in the coastal British Columbia population compared with that in the other three Pacific Northwest populations ($P < .01$; fig. 1*B*), which combined with our previous inference of elevated LD in this population (Jones et al. 2018) could suggest recent inbreeding and population size reduction. We further found a significantly higher proportion of homozygosity for synonymous, nonsynonymous, and nonsense SNPs in the British Columbia population relative to the other populations (fig. 1*C*), which suggests elevated mutational load in British Columbia under a recessive deleterious mutation model. British Columbia individuals also have a significantly higher proportion of strongly deleterious nonsynonymous variants (27.7%; $|s| \geq 10^{-3}$) relative to other populations (0.8%–3.2%; fig. 1*D*; table S2). Because we have the same sample size for Montana and British Columbia ($n = 14$ individuals), this striking difference in the DFE is likely not the result of a relatively small British Columbia sample size, which can lead to overestimation of the proportion of strongly deleterious variation (Kim et al. 2017). Notably, if synonymous SNPs used for demographic inference experience direct or linked selection (e.g., Akashi 1994; Stoletzki and Eyre-Walker 2006; Resch et al. 2007; Pouyet et al. 2018), then our demographic model could be misinferred (Ewing and Jensen 2016; Johri et al. 2020) in such a way that we will underestimate the strength of purifying selection on nonsynonymous SNPs. Regardless, assuming that levels of linked selection are similar across populations, the relative differences we observe in the DFE are unlikely to be driven by weak or linked selection on synonymous variants.

The History of Hybridization and Introgression

From our complete mtDNA assemblies, we estimated a divergence time of 3.299 million generations ago (Mga; 95% highest posterior density [HPD] interval: 2.555–4.255 Mga; fig. 2) between black-tailed jackrabbit and nonintrogressed snowshoe hares, which is consistent with previous estimates of species' split times (Matthee et al. 2004; Melo-Ferreira et al. 2014; Jones et al. 2018). Within the nonintrogressed snowshoe hare mtDNA clade, we found a relatively deep split between the Utah snowshoe hare (representing the "Rockies" cluster identified by Cheng et al. [2014]) and all other snowshoe hares (641 kga; 95% HPD interval: 476–834 kga; fig. 2).

A significant portion of snowshoe hares from the Pacific Northwest (100% of Oregon hares and 50% of Washington hares) formed a reciprocally monophyletic clade relative to black-tailed jackrabbits (100% posterior node support; fig. 2). As previously demonstrated through coalescent simulations (Melo-Ferreira et al. 2014), this phylogenetic pattern cannot be plausibly explained by ILS and is consistent with asymmetric introgression of black-tailed jackrabbit mtDNA into snowshoe hares. As expected, mtDNA was not associated with winter coat color in the Pacific Northwest polymorphic zone (χ^2 $P = 1$). However, if we assume that hybridization is rare, then mtDNA may track the same hybridization event that introduced winter-brown *Agouti* variation into Pacific Northwest hares. The estimated split time between black-tailed jackrabbit and introgressed Pacific Northwest hare mtDNA sequences was 516 kga (95% HPD interval: 381–668 kga; fig. 2). However, this split time does not account for segregating ancestral polymorphism (Arbogast et al. 2002) or unsampled mtDNA variation within black-tailed jackrabbits. If we assume that extant variation in snowshoe hares represents a single mtDNA introgression event, then the TMRCA of introgressed Pacific Northwest snowshoe hare variation suggests a more recent date of mtDNA introgression of ~228 kga (95% HPD interval: 168–301 kga).

Our previous work revealed elevated signatures of genome-wide nuclear admixture presumably coincident with introgression of seasonal camouflage variation (Jones et al. 2018).

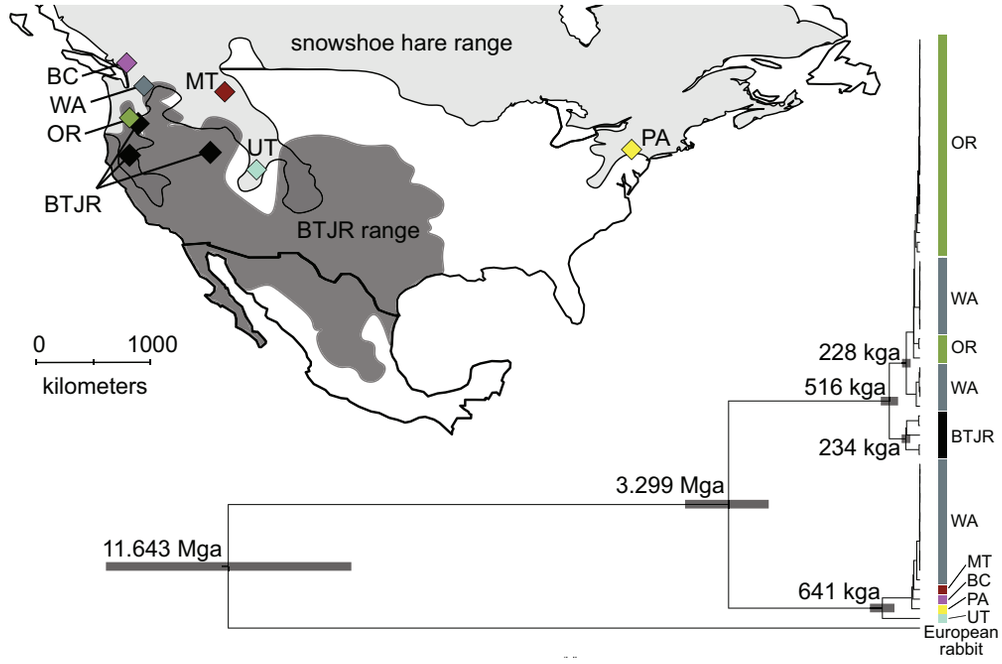

Figure 2: Snowshoe hare and black-tailed jackrabbit (BTJR) ranges with sampling localities for whole-genome sequencing. The phylogenetic tree is a maximum clade credibility tree based on whole mitochondrial genome assemblies (European rabbit as out-group) with median estimated split times for crucial nodes (kga = thousand generations ago; Mga = million generations ago). Sample locality names and colors correspond to those on the map. Gray rectangles show the 95% highest posterior density (HPD) for each node age estimate. BC = British Columbia; MT = Montana; OR = Oregon; PA = Pennsylvania; UT = Utah; WA = Washington.

Here, we identified 1,878 individual introgression tracts with a median length of 28,940 bp, encompassing ~1.99% of the genome (fig. 3). Across single-pulse hybridization scenarios, the most strongly supported age of hybridization was 7–9 kga, with ranges of 95% CIs spanning 6–11 kga (fig. S4). Different rates of admixture or admixture pulse lengths appeared to have little effect on the inferred hybridization age or the overall fit to empirical data (fig. S4). Furthermore, we observed poor model fitting for very recent hybridization (<5 kga). Under a two-pulse hybridization scenario, we infer that the initial pulse of hybridization occurred 14 kga, with a secondary pulse occurring 4 kga (pulses are constrained to be 10,000 generations apart). However, the 95% CI under a two-pulse model spanned 9–15 kga, meaning that in some cases the data best fit a single pulse ~9 kga (before the second simulated pulse). Finally, assuming a scenario of continuous hybridization, our data were most consistent with hybridization beginning 6 kga (100% bootstrap support). However, model fits under continuous hybridization were significantly lower (D = 0.483; 95% quantile: 0.461–0.520) than model fits for hybridization pulses (D = 0.031–0.067; fig. S4), and thus we rejected a continuous hybridization model. We were unable to select an overall best-fit hybridization pulse model, as D statistic values for all pulse models were broadly overlapping (fig. S4).

Positive Selection for Winter-Brown Camouflage

We identified the *Agouti* region as one of the longest (209,012 bp) and most highly supported (mean introgression probability: 0.99) introgression tracts in the Washington winter-brown hare genome (fig. 4). To understand the history of positive selection on brown winter camouflage, we estimated the TMRCA of the selected winter-brown *Agouti* haplotype in snowshoe hares using targeted sequencing across the *Agouti* region (mean coverage per interval: 34× ± 17×). Using a divergent population, a local population, or both to represent the ancestral haplotype had little effect on TMRCA estimates (table S3), so here we present estimates using both populations. Under a low or high estimate of the rabbit mutation rate, we inferred a TMRCA of approximately 1,278 generations (95% CI: 1,135–1,441 generations) or 1,226 generations (95% CI: 1,054–1,408 generations) for the winter-brown Oregon haplotype and approximately 1,392 generations (95% CI: 1,153–1,607 generations) or 972 generations (95% CI: 766–1,169 generations) for the Washington haplotype, respectively (table S3).

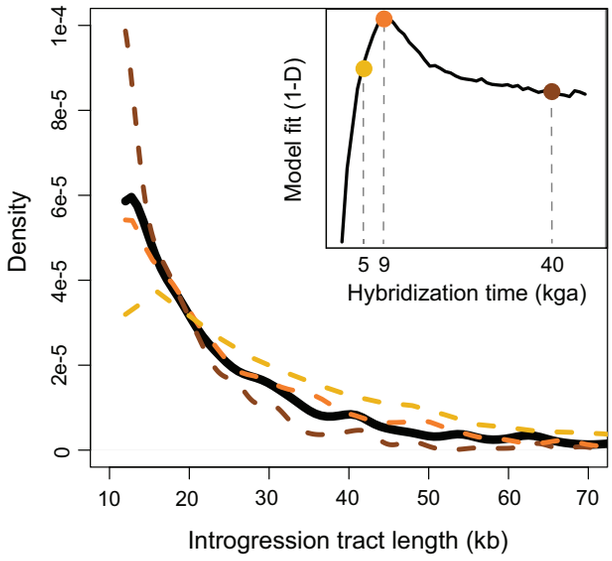

Figure 3: Empirical and simulated distributions of introgression tract lengths in kilobases. The black line shows the empirical distribution of genome-wide introgression tract lengths in snowshoe hares. Colored dashed lines show simulated tract length distributions at three time points following a 100-generation pulse of hybridization at 0.1% frequency (yellow = 5 thousand generations ago [kga]; orange = 9 kga; brown = 40 kga). The inset shows the overall fit of simulated introgression tract lengths to the empirical distribution through time, with hybridization occurring 9 kga as the model with the strongest fit (95% confidence interval: 8–10.5 kga).

We observed no consistent allelic differences between the fixed haplotypes in Washington and Oregon (fig. 4), consistent with a hard selective sweep.

Haplotype-based methods are known to underestimate the TMRCA, and accounting for this systematic error produces TMRCA estimates of approximately 2–4 kga (for a fully recessive allele, $\log_2(\text{estimate}/\text{true}) \approx -1.5$; Kelley 2012) for the winter-brown haplotype in Oregon and Washington. If our estimates are accurate, then there appears to be a ~3,000–12,000 generation lag between the origin of the winter-brown haplotype in snowshoe hares (i.e., the inferred age of initial hybridization date ~7–14 kga) and the increase in frequency of the winter-brown haplotype in the Pacific Northwest from a single copy. Simulations show that long sojourn times and temporal lags are expected for selection on recessive variation; however, the duration of this lag (and the total sojourn time) is negatively associated with the hybridization rate and fixation probability, as expected (table 2). For instance, under the lowest hybridization rate (0.01% for one generation) the time between the origin and TMRCA for a fixed beneficial mutation (i.e., lag time) was 2,140 generations (95% CI: 101–8,322 generations) with only a 0.8% fixation probability, and under the highest hybridization rate (0.1% for 100 generations) the mean lag time was only 625 generations but with 100% fixation probability. Conditional on fixation, increased hybridization rates also tended to be more often associated with soft rather than hard sweeps (e.g., 38% hard sweeps for 0.1% hybridization rate for 100 generations vs. 98% hard sweeps for 0.01% hybridization rate for one generation). However, under intermediate hybridization scenarios (0.1% for one generation or 0.01% for 100 generations), we observed relatively long mean lag times (2,514 and 1,587 generations, respectively) associated with high probabilities of fixation (12% and 79%, respectively), often through hard selective sweeps (81% and 96%; table 2).

Discussion

Range-edge adaptation may enhance a species' evolutionary resilience to environmental change (Hampe and Petit 2005; Hill et al. 2011); however, rigorous population genetic evaluations of predictions for range-edge demography and adaptation are limited (Bridle and Vines 2007). In snowshoe hares, the evolution of brown winter coats in temperate climates along the Pacific Northwest coast represents perhaps the clearest example of local phenotypic adaptation in this wide-ranging species. Given its direct link to reduced snow cover, the evolution of brown winter camouflage may further foster persistence of snowshoe hares in the face of climate change (Mills et al. 2018). Here, we leveraged our understanding of the genetic basis of brown winter camouflage to examine the history of range-edge adaptation, lending insights into the potential for rapid adaptation following environmental change.

Population History and Mutational Load at the Range Edge

Populations along range margins are predicted to be small, limiting their ability to adapt to local conditions (although see Moeller et al. 2011; Graignic et al. 2018). Although we cannot assess relative differences in N_e across the entire hare range, we uncovered high N_e estimates across Pacific Northwest populations (161,654–257,219; table 1), despite evidence for strong ancient population size reductions. Recent theoretical work has demonstrated intrinsic limitations to the accuracy of SFS-based approaches for inferring population size changes (Terhorst and Song 2015), and thus our population size parameter estimates should be interpreted with caution. Moreover, our N_e estimates derive from predictions of genetic drift (i.e., variance N_e) over long evolutionary timescales and may be a weak reflection of current census sizes, especially if local populations experience migration (Wang and Whitlock 2003) or have undergone recent size changes that are undetectable with the SFS (Beichman et al. 2018). We found evidence of significantly

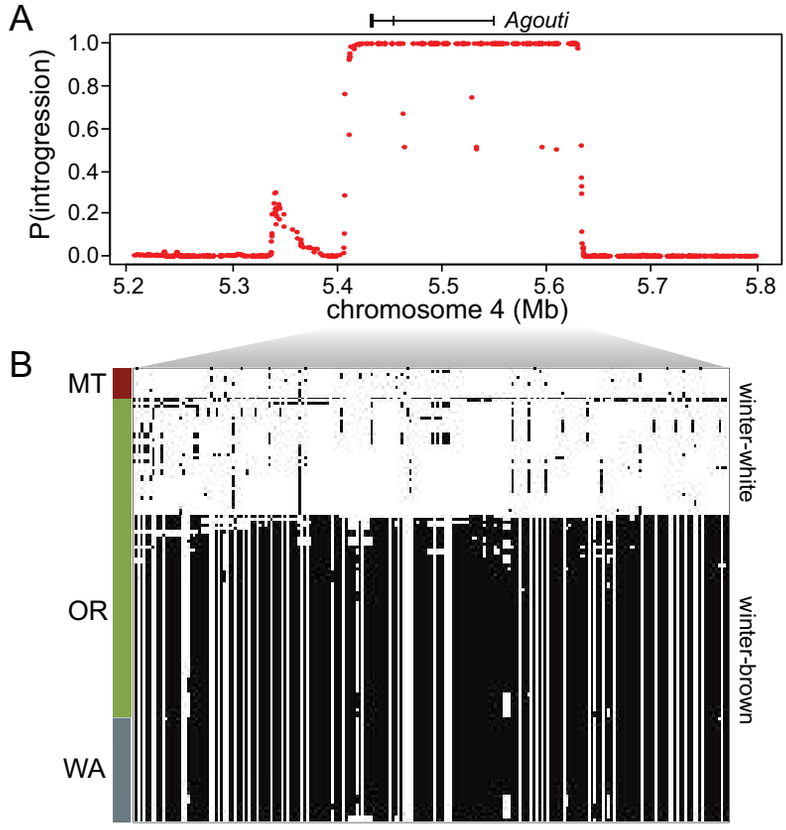

Figure 4: *A*, PhyloNet-HMM (Liu et al. 2014) classification of the probability of introgression for each variable position across the *Agouti* locus. *B*, Haplotype structure across the inferred introgressed *Agouti* interval (chr4:5424111–5633123) for winter-white and winter-brown Pacific Northwest snowshoe hares. MT = Montana; OR = Oregon; WA = Washington.

higher inbreeding coefficients and mutational load in the coastal British Columbia population relative to the inland and montane populations (fig. 1), which may be indicative of a recent population size reduction in British Columbia (Peischl et al. 2013, 2015; Bosshard et al. 2017; Gilbert et al. 2018). Elevated F_{IS} and LD (fig. S1 in Jones et al. 2018) could instead be related to cryptic population substructure (i.e., the Wahlund effect; Waples 2015). However, we have found no evidence for substructure or admixture in British Columbia that could produce this effect (Jones et al. 2020). Similar signatures of elevated mutational load (e.g., homozygosity for deleterious alleles) have been found in other range-front populations, including the plant *Mercurialis annua* (González-Martínez et al. 2017), and in human populations that migrated out of Africa (Henn et al. 2016; although see Simons and Sella 2016). Thus, an intriguing potential explanation for these patterns is that they reflect signatures of a founder event associated with a recent range expansion. Moreover, given that we observe these signatures in the coastal winter-brown population, it is possible that this expansion was enabled by the evolution of locally adaptive brown winter camouflage. Winter-white hares experience heavy predation when mismatched (Zimova et al. 2016) and are not known to occur in low-lying coastal regions west of the Cascade Range (Nagorsen 1983; Mills et al. 2018), suggesting that coastal environments with ephemeral snow cover were likely unoccupied prior to local camouflage adaptation.

Long-term persistence of populations under environmental change ultimately requires adaptive evolution and the ability to colonize novel environments. If the colonization of coastal Pacific Northwest environments by snowshoe hares was enabled by the evolution of brown winter coats, our results underscore that local adaptation to new environments can act as a negative feedback on fitness through the accumulation of deleterious mutations (Pujol and Pannell 2008; Gilbert et al. 2017; González-Martínez et al. 2017; Stewart et al. 2017; Willi et al. 2018). Although the consequences of mutational load for the persistence of Pacific Northwest hare populations are unclear, high recessive mutational load may compromise the adaptive potential of populations (Assaf et al. 2015; González-Martínez et al. 2017) and increase the probability of extinction in small

Table 2: Results from simulations of positive selection on recessive variation

	1-generation pulse		100-generation pulse	
	.01%	.1%	.01%	.1%
P(fixation)	.0082	.12	.79	1.0
	(.0068–.010)	(.098–.13)	(.71–.85)	(.96–1.0)
P(hard sweep)	.98	.81	.96	.38
	(.93–.99)	(.72–.87)	(.90–.98)	(.29–.48)
T(sojourn)	8,911	9,448	6,472	5,612
	(5,179–16,208)	(5,626–15,746)	(5,088–15,339)	(4,319–6,757)
T(lag)	2,140	2,514	1,587	624
	(101–8,322)	(97–7,740)	(87–7,253)	(91–1,899)

Note: The beneficial variant was introduced through hybridization during a 1- or 100-generation pulse at a rate of 0.01% or 0.1%. Data are shown for the probability of fixation (*P*(fixation)) and, conditional on fixation, the probability of a hard selective sweep (*P*(hard sweep)), the mean sojourn time (*T*(sojourn)), and the mean lag time between a fixed mutation's origin and the time to the most recent common ancestor (*T*(lag)). In parentheses are 95% confidence intervals.

populations (Mills and Smouse 1994; Frankham 1998). In experiments of isolated *Tribolium* populations, short-term fitness gains via adaptive evolution were entirely lost over longer time periods as a consequence of increasing mutational load, although fitness could be readily restored through admixture (Stewart et al. 2017). In snowshoe hares, the potential fitness costs linked to mutational load may be mitigated by high gene flow between populations (table S1) or superseded by the enhanced species-level evolutionary resilience afforded by brown winter camouflage during periods of low snow cover. Regardless, we suggest that any conservation efforts to promote adaptation to climate change should weigh the potential for enhanced long-term population persistence against the potential short-term fitness costs that may arise through mutational load.

Hybridization and the Origin of the Winter-Brown Allele

Hybridization may play an important role in shaping adaptation and expansion of range-edge populations (Pfennig et al. 2016), but evidence for this mode of adaptation stems from only a handful of examples (e.g., Lewontin and Birch 1966; Besansky et al. 2003; Rieseberg et al. 2007). In snowshoe hares, range and niche expansion into mild Pacific Northwest coastal environments appears to have been enabled by adaptive introgression, although the history of hybridization has remained unclear. We estimated that mtDNA introgression in Pacific Northwest snowshoe hares occurred ~228 kga, which could be interpreted as a conservative upper bound for the timing of hybridization with black-tailed jackrabbits. Meanwhile, the genome-wide distribution of introgression tract lengths, which should be less sensitive to ILS and population structure within hares (Liu et al. 2014), suggest a much more recent pulse or pulses of hybridization starting no more than 14 kga (figs. 3, S5). The different nuclear DNA–based and mtDNA-based estimates may also reflect independent pulses of ancient hybridization. Severe systematic overestimation of divergence dates may be common with mtDNA genomes calibrated using a relatively divergent out-group because of high mutation rates and substitution saturation (Zheng et al. 2011). The divergence dates among major snowshoe hare mtDNA lineages also appear to be much deeper than our best estimates derived from population (nuclear) genomic data (about two- to threefold deeper; Jones et al. 2020), which suggests that our analyses based on mtDNA likely overestimate the timing of introgression. We assumed a relatively simple molecular clock model, and more complicated models (e.g., relaxed clocks) might better account for mutational processes observed in mtDNA genomes. However, it would seem that there would be little insight to be gained by additional modeling here given the myriad limitations associated with extrapolating population history from a single stochastic realization of the coalescent process (Hudson and Turelli 2003).

Several recent studies have also noted that introgression is often positively correlated with local recombination rate (Nachman and Payseur 2012; Janoušek et al. 2015; Schumer et al. 2018; Edelman et al. 2019; Li et al. 2019; Martin et al. 2019), presumably due to the effects of linked selection against deleterious mutations in hybrids. If this relationship generally holds, then it is possible that our dating approach based on the distribution of introgression tract lengths is also upwardly biased. However, contemporary range overlap between snowshoe hares and black-tailed jackrabbits appears to be restricted to relatively sharp ecological transitions between sage scrub and montane forests in Oregon and California (fig. 2) and no records of putative hybrids exist, suggesting that contemporary or very recent hybridization (e.g., <1,000 generations ago) is likely exceedingly rare or absent and has not resulted in discernible gene flow. Notably, our estimates of the age of genome-wide admixture, assuming one to two generations per year in hares (Marboutin and Peroux 1995), appears to be coincident with the retreat of the Cordilleran ice sheet from low-lying coastal

habitats in southern British Columbia and northern Washington at the end of the last glacial maximum (~18,000 years ago; Darvill et al. 2018) and thus the opening of suitable habitat for winter-brown snowshoe hares. This period of rapid climatic change resulted in individualistic range shifts for many North American mammal species (Graham 1986), potentially leading to novel community assemblages and thus promoting hybridization events (Swenson and Howard 2005), which could have created conditions favorable to adaptive introgression.

The Spread of Winter-Brown Camouflage and the Tempo of Local Adaptation

Although theory predicts that adaptation in small range-edge populations may be slow and mutation limited, hybridization may alleviate the lack of beneficial variation along range margins (Pfennig et al. 2016). Revealing how introgressed alleles adaptively spread through populations is therefore a critical component of understanding the limitations of range-edge adaptation. Here, we identified *Agouti* as one of the largest (>200 kb) and most strongly supported introgression tracts genome-wide (fig. 4), consistent with our previous study showing exceptionally low absolute genetic divergence in this genomic region between black-tailed jackrabbits and winter-brown snowshoe hares (Jones et al. 2018). Assuming our genome-wide estimates of the initial age of hybridization (either one or two pulses) reflect the origin of the *Agouti* allele through introgression (~7–14 kga), our findings suggest a ~3,000–12,000 generation delay from the onset of hybridization until the selective sweep (i.e., TMRCA) of the winter-brown haplotype in the Pacific Northwest.

One potential biological explanation for this temporal lag is that winter-brown camouflage was not immediately beneficial in snowshoe hares. Rather, the winter-brown variant may have initially segregated as a neutral or deleterious allele for a period of time until an environmental shift allowed positive selection to act quickly on standing variation (e.g., Colosimo et al. 2005). However, our simulations suggest that beneficial recessive alleles segregating at frequencies as high as ~10% (equivalent to simulations of a 0.1% hybridization rate for 100 generations) take on average ~5,612 generations (95% CI: 4,319–6,757 generations) to reach fixation (table 2). Thus, under an environmental shift scenario, the starting frequency of the winter-brown variant would likely have to be quite large (>10%) in order for selection to quickly drive it to fixation. Although allelic fixation under this model would be virtually guaranteed (table 2), we suspect that such a high level of hybridization between black-tailed jackrabbits and snowshoe hares is unlikely given their ecological distinctiveness and our estimate of the genome-wide proportion of introgression (~1.99%). Furthermore, the high starting allele frequency needed to result in rapid fixation is at odds with the evidence that selection fixed a single haplotype, as higher hybridization rates tended to result in softer sweeps (table 2).

An alternative explanation for the delayed rise in frequency of the winter-brown allele invokes the limits of positive selection on recessive variation, which is predicted to result in an extended period of drift while at low frequency until homozygous recessive genotypes become more common. Consistent with this, we found long sojourn times and significant temporal lags between the timing of hybridization and the TMRCA of fixed beneficial recessive alleles under low and moderate rates of hybridization (table 2). Under a two-pulse hybridization model (fig. S4), it is plausible that introgressed variation at *Agouti* was lost following an initial pulse and was then reintroduced via a more recent introgression event ~4 kga. Such a scenario would reconcile an apparent delay between the inferred timing of hybridization and the TMRCA of the selective sweep, but it would also require rapid fixation of the recessive *Agouti* haplotype on a timescale that our simulations suggest are extremely unlikely (e.g., T(sojourn) 95% CI lower bound: 4,319–5,626 generations across hybridization models; see table 2). Although fixation under our lowest simulated rate of hybridization was highly unlikely (~0.8%; table 2), the two intermediate scenarios still resulted in relatively high fixation probabilities (12%–78%) and tended to produce hard sweeps (81%–96%), consistent with observed patterns of genetic variation at the winter-brown *Agouti* haplotype. Collectively, these results suggest that the lag between the origin and the selective sweep of the winter-brown allele can largely be explained by the limits of natural selection on beneficial recessive variation introduced through hybridization at low to moderate frequency (~0.1%–1%). Indeed, this mutation-limited scenario is consistent with other known instances of colonization of novel environments through the evolution of locally adaptive camouflage in Nebraska deer mice and White Sands lizards (Laurent et al. 2016; Pfeifer et al. 2018; Harris et al. 2020). However, we are unable to completely rule out a scenario in which a portion of the total temporal lag is explained by the winter-brown allele segregating as a neutral or deleterious variant for a period of time.

Rates of adaptation at range edges are potentially an important component of species' responses to climate change (Hampe and Petit 2005). Our study highlights the key role that hybridization can play in seeding adaptive variation and facilitating range expansion during periods of environmental change. In some cases, introgression appears to facilitate very rapid adaptation to environmental change (Norris et al. 2015; Oziolor et al. 2019). However, introgression may not always be an efficient solution for rapid adaptation, as here we demonstrate that the rate of adaptation to novel mild winter environments in snowshoe hares appears

to have been limited by the dominance coefficient of the winter-brown allele. Collectively, our findings demonstrate key factors that promote and limit adaptation to changing environments and in particular highlight the importance of characterizing genetic dominance of beneficial variants for understanding rates of adaptation and range expansion under climate change.

Acknowledgments

We thank E. Cheng and K. Garrison for assistance with sample collection. We thank J. Melo-Ferreira, P. C. Alves, M. S. Ferreira, N. Herrera, E. Kopania, A. Kumar, M. Zimova, K. Garrison, N. Edelman, M. Hahn, and the UNVEIL network for helpful discussions. We thank B. Kim for assistance with Fitδaδi analysis. Funding and support for this research was provided a National Science Foundation (NSF) Graduate Research Fellowship (DGE-1313190), a NSF Doctoral Dissertation Improvement Grant (DGE-1702043), NSF Graduate Research Opportunities Worldwide, the NSF Established Program to Stimulate Competitive Research (EPSCoR; OIA-1736249), the NSF (DEB-0841884; DEB-1907022), the Drollinger-Dial Foundation, an American Society of Mammalogists Grant-in-Aid of Research, and a Swiss Government Excellence Scholarship.

Statement of Authorship

M.R.J., J.M.G., and L.S.M. conceived and designed the study and obtained funding; L.S.M. led all fieldwork and related collection of biological samples; M.R.J. performed molecular laboratory work, data analysis, and data visualization with contributions and guidance from J.M.G. and J.D.J.; and M.R.J. led the writing with contributions from all authors. All authors gave final approval for publication and agree to be held accountable for the work performed therein.

Data and Code Availability

Original sequence data are available in the Sequence Read Archive (www.ncbi.nlm.nih.gov/sra) under BioProject PRJNA420081 (SAMN13999419-13999472). Supporting data files and scripts have been deposited in the Dryad Digital Repository (https://doi.org/10.5061/dryad.8gtht76km; Jones 2020).

Literature Cited

Ackerly, D. D. 2003. Community assembly, niche conservatism, and adaptive evolution in changing environments. International Journal of Plant Sciences 164:S165–S184.

Akashi, H. 1994. Synonymous codon usage in *Drosophila melanogaster*: natural selection and translational accuracy. Genetics 136:927–935.

Antonovics, J. 1976. The nature of limits to natural selection. Annals of the Missouri Botanical Garden 63:224–247.

Arbogast, B. S., S. V. Edwards, J. Wakeley, P. Beerli, and J. B. Slowinski. 2002. Estimating divergence times from molecular data on phylogenetic and population genetic timescales. Annual Review of Ecology and Systematics 33:707–740.

Assaf, Z. J., D. A. Petrov, and J. R. Blundell. 2015. Obstruction of adaptation in diploids by recessive, strongly deleterious alleles. Proceedings of the National Academy of Sciences of the USA 112:E2658–E2666.

Baker, H. G. 1948. Stages in invasion and replacement demonstrated by species of *Melandrium*. Journal of Ecology 36:96–119.

Barton, N. 2001. Adaptation at the edge of a species' range. Pages 365–392 *in* J. Silvertown and J. Antonovics, eds. Integrating ecology and evolution in a spatial context. Blackwell Science, Oxford.

Behrman, K. D., and M. Kirkpatrick. 2011. Species range expansion by beneficial mutations. Journal of Evolutionary Biology 24:665–675.

Beichman, A. C., E. Huerta-Sanchez, and K. E. Lohmueller. 2018. Using genomic data to infer historic population dynamics of nonmodel organisms. Annual Review of Ecology, Evolution, and Systematics 49:433–456.

Besansky, N. J., J. Krzywinski, T. Lehmann, F. Simard, M. Kern, O. Mukabayire, D. Fontenille, et al. 2003. Semipermeable species boundaries between *Anopheles gambiae* and *Anopheles arabiensis*: evidence from multilocus DNA sequence variation. Proceedings of the National Academy of Sciences of the USA 100:10818–10823.

Bolger, A. M., M. Lohse, and B. Usadel. 2014. Trimmomatic: a flexible trimmer for Illumina sequence data. Bioinformatics 30:2114–2120.

Bontrager, M., and A. L. Angert. 2019. Gene flow improves fitness at a range edge under climate change. Evolution Letters 3:55–68.

Bosshard, L., I. Dupanloup, O. Tenaillon, R. Bruggmann, M. Ackermann, S. Peischl, and L. Excoffier. 2017. Accumulation of deleterious mutations during bacterial range expansions. Genetics 207:669–684.

Bouckaert, R., J. Heled, D. Kühnert, T. Vaughan, C.-H. Wu, D. Xie, M. A. Suchard, et al. 2014. BEAST 2: a software platform for Bayesian evolutionary analysis. PLoS Computational Biology 10:e1003537.

Bridle, J. R., and T. H. Vines. 2007. Limits to evolution at range margins: when and why does adaptation fail? Trends in Ecology and Evolution 22:140–147.

Browning, S. R., and B. L. Browning. 2007. Rapid and accurate haplotype phasing and missing-data inference for whole-genome association studies by use of localized haplotype clustering. American Journal of Human Genetics 81:1084–1097.

Burke, J. M., and M. L. Arnold. 2001. Genetics and the fitness of hybrids. Annual Review of Genetics 35:31–52.

Carneiro, M., S. Afonso, A. Geraldes, H. Garreau, G. Bolet, S. Boucher, A. Tircazes, et al. 2011. The genetic structure of domestic rabbits. Molecular Biology and Evolution 28:1801–1816.

Carneiro, M., F. W. Albert, J. Melo-Ferreira, N. Galtier, P. Gayral, J. A. Blanco-Aguiar, R. Villafuerte, et al. 2012. Evidence for widespread positive and purifying selection across the European rabbit (*Oryctolagus cuniculus*) genome. Molecular Biology and Evolution 29:1837–1849.

Carneiro, M., C.-J. Rubin, F. Di Palma, F. W. Albert, J. Alföldi, A. Martinez Barrio, G. Pielberg, et al. 2014. Rabbit genome analysis reveals a polygenic basis for phenotypic change during domestication. Science 345:1074–1079.

Cheng, E., K. E. Hodges, J. Melo-Ferreira, P. C. Alves, and L. S. Mills. 2014. Conservation implications of the evolutionary history and genetic diversity hotspots of the snowshoe hare. Molecular Ecology 23:2929–2942.

Cingolani, P., A. Platts, L. L. Wang, M. Coon, T. Nguyen, L. Wang, S. J. Land, et al. 2012. A program for annotating and predicting the effects of single nucleotide polymorphisms, SnpEff: SNPs in the genome of *Drosophila melanogaster* strain w1118; iso-2; iso-3. Fly 6:80–92.

Coffman, A. J., P. H. Hsieh, S. Gravel, and R. N. Gutenkunst. 2016. Computationally efficient composite likelihood statistics for demographic inference. Molecular Biology and Evolution 33:591–593.

Colosimo, P. F., K. E. Hosemann, S. Balabhadra, G. Villarreal, M. Dickson, J. Grimwood, J. Schmutz, et al. 2005. Widespread parallel evolution in sticklebacks by repeated fixation of *Ectodysplasin* alleles. Science 307:1928–1933.

Corbett-Detig, R., and M. Jones. 2016. SELAM: simulation of epistasis and local adaptation during admixture with mate choice. Bioinformatics 32:3035–3037.

Danecek, P., A. Auton, G. Abecasis, C. A. Albers, E. Banks, M. A. DePristo, R. E. Handsaker, et al. 2011. The variant call format and VCFtools. Bioinformatics 27:2156–2158.

Darvill, C. M., B. Menounos, B. M. Goehring, O. B. Lian, and M. W. Caffee. 2018. Retreat of the western Cordilleran Ice Sheet margin during the last deglaciation. Geophysical Research Letters 45:9710–9720.

Dierckxsens, N., P. Mardulyn, and G. Smits. 2017. NOVOPlasty: de novo assembly of organelle genomes from whole genome data. Nucleic Acids Research 45:e18.

Edelman, N. B., P. B. Frandsen, M. Miyagi, B. J. Clavijo, J. Davey, R. Dikow, G. Garcia-Accinelli, et al. 2019. Genomic architecture and introgression shape a butterfly radiation. Science 366:594–599.

Ewing, G. B., and J. D. Jensen. 2016. The consequences of not accounting for background selection in demographic inference. Molecular Ecology 25:135–141.

Forsman, A. 2016. Is colour polymorphism advantageous to populations and species? Molecular Ecology 25:2693–2698.

Frankham, R. 1998. Inbreeding and extinction: island populations. Conservation Biology 12:665–675.

Garcia-Ramos, G., and M. Kirkpatrick. 1997. Genetic models of adaptation and gene flow in peripheral populations. Evolution 51:21–28.

Gilbert, K. J., S. Peischl, and L. Excoffier. 2018. Mutation load dynamics during environmentally-driven range shifts. PLoS Genetics 14:e1007450.

Gilbert, K. J., N. P. Sharp, A. L. Angert, G. L. Conte, J. A. Draghi, F. Guillaume, A. L. Hargreaves, et al. 2017. Local adaptation interacts with expansion load during range expansion: maladaptation reduces expansion load. American Naturalist 189:368–380.

Gilbert, K. J., and M. C. Whitlock. 2016. The genetics of adaptation to discrete heterogeneous environments: frequent mutation or large-effect alleles can allow range expansion. Journal of Evolutionary Biology 30:591–602.

González-Martínez, S. C., K. Ridout, and J. R. Pannell. 2017. Range expansion compromises adaptive evolution in an outcrossing plant. Current Biology 27:2544–2551.

Graham, R. W. 1986. Response of mammalian communities to environmental changes during the late Quaternary. Pages 300–313 *in* J. Diamond and T. J. Case, eds. Community ecology. Harper & Row, New York.

Graignic, N., F. Tremblay, and Y. Bergeron. 2018. Influence of northern limit range on genetic diversity and structure in a widespread North American tree, sugar maple (*Acer saccharum* Marshall). Ecology and Evolution 8:2766–2780.

Griffin, P. C., and L. S. Mills. 2009. Sinks without borders: snowshoe hare dynamics in a complex landscape. Oikos 118:1487–1498.

Gutenkunst, R. N., R. D. Hernandez, S. H. Williamson, and C. D. Bustamante. 2009. Inferring the joint demographic history of multiple populations from multidimensional SNP frequency data. PLoS Genetics 5:e1000695.

Haldane, J. B. S. 1924. A mathematical theory of natural and artificial selection part I. Transactions of the Cambridge Philosophical Society 23:19–41.

———. 1930. A mathematical theory of natural and artificial selection (part VI, isolation). Mathematical Proceedings of the Cambridge Philosophical Society 26:220–230.

Haller, B. C., J. Galloway, J. Kelleher, P. W. Messer, and P. L. Ralph. 2019. Tree-sequence recording in SLiM opens new horizons for forward-time simulations of whole genomes. Molecular Ecology Resources 19:552–566.

Haller, B. C., and P. W. Messer. 2019. SLiM 3: forward genetic simulations beyond the Wright-Fisher model. Molecular Biology and Evolution 36:632–637.

Hampe, A., and R. J. Petit. 2005. Conserving biodiversity under climate change: the rear edge matters. Ecology Letters 8:461–467.

Harris, R. B., K. Irwin, M. R. Jones, S. Laurent, R. D. H. Barrett, R. D. H. Nachman, J. M. Good, et al. 2020. The population genetics of crypsis in vertebrates: recent insights from mice, hares, and lizards. Heredity 124:1–14.

Hedrick, P. W. 2013. Adaptive introgression in animals: examples and comparison to new mutation and standing variation as sources of adaptive variation. Molecular Ecology 22:4606–4618.

Henn, B. M., L. R. Botigué, S. Peischl, I. Dupanloup, M. Lipatov, B. K. Maples, A. R. Martin, et al. 2016. Distance from sub-Saharan Africa predicts mutational load in diverse human genomes. Proceedings of the National Academy of Sciences of the USA 113:E440–E449.

Hill, J. K., H. M. Griffiths, and C. D. Thomas. 2011. Climate change and evolutionary adaptations at species' range margins. Annual Review of Entomology 56:143–159.

Holt, R. D., and R. Gomulkiewicz. 1997. How does immigration influence local adaptation? a reexamination of a familiar paradigm. American Naturalist 149:563–572.

Hudson, R. R., and M. Turelli. 2003. Stochasticity overrules the "three-times rule": genetic drift, genetic draft, and coalescence times for nuclear loci versus mitochondrial DNA. Evolution 57:182–190.

Huerta-Sánchez, E., X. Jin, Asan, Z. Bianba, B. M. Peter, N. Vinckenbosch, Y. Liang, et al. 2014. Altitude adaptation in Tibetans caused by introgression of Denisovan-like DNA. Nature 512:194–197.

Janoušek, V., P. Munclinger, L. Wang, K. C. Teeter, and P. K. Tucker. 2015. Functional organization of the genome may shape the species boundary in the house mouse. Molecular Biology and Evolution 32:1208–1220.

Johri, P., B. Charlesworth, and J. D. Jensen. 2020. Toward an evolutionarily appropriate null model: jointly inferring demography and purifying selection. Genetics 215:173–192.

Jones, M. R., L. S. Mills, J. D. Jensen, and J. M. Good. 2020. Data from: The origin and spread of locally adaptive seasonal

camouflage in snowshow hares. American Naturalist, Dryad Digital Repository, https://doi.org/10.5061/dryad.8gtht76km.

Jones, M. R., L. S. Mills, P. C. Alves, C. M. Callahan, J. M. Alves, D. J. R. Lafferty, F. M. Jiggins, et al. 2018. Adaptive introgression underlies polymorphic seasonal camouflage in snowshoe hares. Science 360:1355–1358.

Jones, M. R., L. S. Mills, J. D. Jensen, and J. M. Good. 2020. Convergent evolution of seasonal camouflage in response to reduced snow cover across the snowshoe hare range. Evolution, https://doi.org/10.1111/evo.13976.

Kawecki, T. J. 2008. Adaptation to marginal habitats. Annual Review of Ecology, Evolution, and Systematics 39:321–342.

Keightley, P. D., and A. Eyre-Walker. 2010. What can we learn about the distribution of fitness effects of new mutations from DNA sequence data? Philosophical Transactions of the Royal Society B 365:1187–1193.

Kelleher, J., A. M. Etheridge, and G. McVean. 2016. Efficient coalescent simulation and genealogical analysis for large sample sizes. PLoS Computational Biology 12:e1004842.

Kelley, J. L. 2012. Systematic underestimation of the age of selected alleles. Frontiers in Genetics 3:165.

Kim, B. Y., C. D. Huber, and K. E. Lohmueller. 2017. Inference of the distribution of selection coefficients for new nonsynonymous mutations using large samples. Genetics 206:345–361.

Kirkpatrick, M., and N. H. Barton. 1997. Evolution of a species' range. American Naturalist 150:1–23.

Lamichhaney, S., J. Berglund, M. S. Almén, K. Maqbool, M. Grabherr, A. Martinez-Barrio, M. Promerová, et al. 2015. Evolution of Darwin's finches and their beaks revealed by genome sequencing. Nature 518:371–375.

Larkin, M. A., G. Blackshields, N. P. Brown, R. Chenna, P. A. McGettigan, H. McWilliam, F. Valentin, et al. 2007. Clustal W and Clustal X version 2.0. Bioinformatics 23:2947–2948.

Laurent, S., S. P. Pfeifer, M. L. Settles, S. S. Hunter, K. M. Hardwick, L. Ormond, V. C. Sousa, et al. 2016. The population genomics of rapid adaptation: disentangling signatures of selection and demography in White Sands lizards. Molecular Ecology 25:306–323.

Lewontin, R. C., and L. C. Birch. 1966. Hybridization as a source of variation for adaptation to new environments. Evolution 20:315–336.

Li, G., H. V Figueiró, E. Eizirik, and W. J. Murphy. 2019. Recombination-aware phylogenomics reveals the structured genomic landscape of hybridizing cat species. Molecular Biology and Evolution 36:2111–2126.

Li, H. 2013. Aligning sequence reads, clone sequences and assembly contigs with BWA-MEM. arXiv, 1303.3997.

Liu, K. J., J. Dai, K. Truong, Y. Song, M. H. Kohn, and L. Nakhleh. 2014. An HMM-based comparative genomic framework for detecting introgression in eukaryotes. PLoS Computational Biology 10:e1003649.

Loh, P.-R., M. Lipson, N. Patterson, P. Moorjani, J. K. Pickrell, D. Reich, and B. Berger. 2013. Inferring admixture histories of human populations using linkage disequilibrium. Genetics 193:1233–1254.

Lynch, M., J. Conery, and R. Burger. 1995. Mutation accumulation and the extinction of small populations. American Naturalist 146:489–518.

Magoč, T., and S. L. Salzberg. 2011. FLASH: fast length adjustment of short reads to improve genome assemblies. Bioinformatics 27:2957–2963.

Marboutin, E., and R. Peroux. 1995. Survival pattern of European hare in a decreasing population. Journal of Applied Ecology 32:809–816.

Marnetto, D., and E. Huerta-Sánchez. 2017. Haplostrips: revealing population structure through haplotype visualization. Methods in Ecology and Evolution 8:1389–1392.

Martin, S. H., J. Davey, C. Salazar, and C. Jiggins. 2019. Recombination rate variation shapes barriers to introgression across butterfly genomes. PLoS Biology 17:e2006288.

Massey, F. J. 1951. The Kolmogorov-Smirnov test for goodness of fit. Journal of the American Statistical Association 46:68–78.

Matthee, C. A., B. J. Van Vuuren, D. Bell, and T. J. Robinson. 2004. A molecular supermatrix of the rabbits and hares (Leporidae) allows for the identification of five intercontinental exchanges during the Miocene. Systematic Biology 53:433–447.

McKenna, A., M. Hanna, E. Banks, A. Sivachenko, K. Cibulskis, A. Kernytsky, K. Garimella, et al. 2010. The genome analysis toolkit: a MapReduce framework for analyzing next-generation DNA sequencing data. Genome Research 20:1297–1303.

Melo-Ferreira, J., F. A. Seixas, E. Cheng, L. S. Mills, and P. C. Alves. 2014. The hidden history of the snowshoe hare, *Lepus americanus*: extensive mitochondrial DNA introgression inferred from multilocus genetic variation. Molecular Ecology 23:4617–4630.

Meyer, M., and M. Kircher. 2010. Illumina sequencing library preparation for highly multiplexed target capture and sequencing. Cold Spring Harbor Protocols 5:pdb.prot5448.

Miao, B., Z. Wang, and Y. Li. 2016. Genomic analysis reveals hypoxia adaptation in the Tibetan mastiff by introgression of the grey wolf from the Tibetan Plateau. Molecular Biology and Evolution 34:734–743.

Mills, L. S., E. V. Bragina, A. V. Kumar, M. Zimova, D. J. R. Lafferty, J. Feltner, B. M. Davis, et al. 2018. Winter color polymorphisms identify global hot spots for evolutionary rescue from climate change. Science 359:1033–1036.

Mills, L. S., and P. E. Smouse. 1994. Demographic consequences of inbreeding in remnant populations. American Naturalist 144:412–431.

Mills, L. S., M. Zimova, J. Oyler, S. Running, J. T. Abatzoglou, and P. M. Lukacs. 2013. Camouflage mismatch in seasonal coat color due to decreased snow duration. Proceedings of the National Academy of Sciences of the USA 110:7360–7365.

Moeller, D. A., M. A. Geber, and P. Tiffin. 2011. Population genetics and the evolution of geographic range limits in an annual plant. American Naturalist 178:S44–S61.

Nachman, M. W., and B. A. Payseur. 2012. Recombination rate variation and speciation: theoretical predictions and empirical results from rabbits and mice. Philosophical Transactions of the Royal Society B 367:409–421.

Nagorsen, D. W. 1983. Winter pelage colour in snowshoe hares (*Lepus americanus*) from the Pacific Northwest. Canadian Journal of Zoology 61:2313–2318.

Nelson, T. C., M. R. Jones, J. P. Velotta, A. S. Dhawanjewar, and R. M. Schweizer. 2019. UNVEILing connections between genotype, phenotype, and fitness in natural populations. Molecular Ecology 28:1866–1876.

Norris, L. C., B. J. Main, Y. Lee, T. C. Collier, A. Fofana, A. J. Cornel, and G. C. Lanzaro. 2015. Adaptive introgression in an African malaria mosquito coincident with the increased usage of insecticide-treated bed nets. Proceedings of the National Academy of Sciences of the USA 112:815–820.

Orr, H. A., and A. J. Betancourt. 2001. Haldane's sieve and adaptation from the standing genetic variation. Genetics 157:875–884.

Oziolor, E. M., N. M. Reid, S. Yair, K. M. Lee, S. Guberman VerPloeg, P. C. Bruns, J. R. Shaw, et al. 2019. Adaptive introgression enables evolutionary rescue from extreme environmental pollution. Science 364:455–457.

Pardo-Diaz, C., C. Salazar, S. W. Baxter, C. Merot, W. Figueiredo-Ready, M. Joron, W. O. McMillan, et al. 2012. Adaptive introgression across species boundaries in *Heliconius* butterflies. PLoS Genetics 8:e1002752.

Peischl, S., I. Dupanloup, M. Kirkpatrick, and L. Excoffier. 2013. On the accumulation of deleterious mutations during range expansions. Molecular Ecology 22:5972–5982.

Peischl, S., M. Kirkpatrick, and L. Excoffier. 2015. Expansion load and the evolutionary dynamics of a species range. American Naturalist 185:E81–E93.

Pfeifer, S. P., S. Laurent, V. C. Sousa, C. R. Linnen, M. Foll, L. Excoffier, H. E. Hoekstra, et al. 2018. The evolutionary history of Nebraska deer mice: local adaptation in the face of strong gene flow. Molecular Biology and Evolution 35:792–806.

Pfennig, K. S., A. L. Kelly, and A. A. Pierce. 2016. Hybridization as a facilitator of species range expansion. Proceedings of the Royal Society B: Biological Sciences 283:20161329.

Polechová, J. 2018. Is the sky the limit? on the expansion threshold of a species' range. PLoS Biology 16:e2005372.

Pouyet, F., S. Aeschbacher, A. Thiéry, and L. Excoffier. 2018. Background selection and biased gene conversion affect more than 95% of the human genome and bias demographic inferences. eLife 7:e36317.

Pujol, B., and J. R. Pannell. 2008. Reduced responses to selection after species range expansion. Science 321:96.

R Core Team. 2018. R: a language and environment for statistical computing. R Foundation for Statistical Computing, Vienna.

Resch, A. M., L. Carmel, L. Mariño-Ramírez, A. Y. Ogurtsov, S. A. Shabalina, I. B. Rogozin, and E. V. Koonin. 2007. Widespread positive selection in synonymous sites of mammalian genes. Molecular Biology and Evolution 24:1821–1831.

Rieseberg, L. H., S.-C. Kim, R. A. Randell, K. D. Whitney, B. L. Gross, C. Lexer, and K. Clay. 2007. Hybridization and the colonization of novel habitats by annual sunflowers. Genetica 129:149–165.

Robinson, J. D., A. J. Coffman, M. J. Hickerson, and R. N. Gutenkunst. 2014. Sampling strategies for frequency spectrum-based population genomic inference. BMC Evolutionary Biology 14:254.

Rohland, N., and D. Reich. 2012. Cost-effective, high-throughput DNA sequencing libraries for multiplexed target capture. Genome Research 22:939–946.

Schumer, M., R. Cui, D. L. Powell, G. G. Rosenthal, and P. Andolfatto. 2016. Ancient hybridization and genomic stabilization in a swordtail fish. Molecular Ecology 25:2661–2679.

Schumer, M., C. Xu, D. L. Powell, A. Durvasula, L. Skov, C. Holland, J. C. Blazier, et al. 2018. Natural selection interacts with recombination to shape the evolution of hybrid genomes. Science 360:656–660.

Sgrò, C. M., A. J. Lowe, and A. A. Hoffmann. 2011. Building evolutionary resilience for conserving biodiversity under climate change. Evolutionary Applications 4:326–337.

Simons, Y. B., and G. Sella. 2016. The impact of recent population history on the deleterious mutation load in humans and close evolutionary relatives. Current Opinion in Genetics and Development 41:150–158.

Slatyer, R. A., M. Hirst, and J. P. Sexton. 2013. Niche breadth predicts geographical range size: a general ecological pattern. Ecology Letters 16:1104–1114.

Smith, J., G. Coop, M. Stephens, and J. Novembre. 2018. Estimating time to the common ancestor for a beneficial allele. Molecular Biology and Evolution 35:1003–1017.

Song, Y., S. Endepols, N. Klemann, D. Richter, F.-R. Matuschka, C.-H. Shih, M. W. Nachman, et al. 2011. Adaptive introgression of anticoagulant rodent poison resistance by hybridization between old world mice. Current Biology 21:1296–1301.

Stamatakis, A. 2014. RAxML version 8: a tool for phylogenetic analysis and post-analysis of large phylogenies. Bioinformatics 30:1312–1313.

Stewart, G. S., M. R. Morris, A. B. Genis, M. Szűcs, B. A. Melbourne, S. J. Tavener, and R. A. Hufbauer. 2017. The power of evolutionary rescue is constrained by genetic load. Evolutionary Applications 10:731–741.

Stoletzki, N., and A. Eyre-Walker. 2006. Synonymous codon usage in *Escherichia coli*: selection for translational accuracy. Molecular Biology and Evolution 24:374–381.

Swenson, N. G., and D. J. Howard. 2005. Clustering of contact zones, hybrid zones, and phylogeographic breaks in North America. American Naturalist 166:581–591.

Taylor, S. A., and E. L. Larson. 2019. Insights from genomes into the evolutionary importance and prevalence of hybridization in nature. Nature Ecology and Evolution 3:170–177.

Terhorst, J., and Y. S. Song. 2015. Fundamental limits on the accuracy of demographic inference based on the sample frequency spectrum. Proceedings of the National Academy of Sciences of the USA 112:7677–7682.

Teshima, K. M., and M. Przeworski. 2006. Directional positive selection on an allele of arbitrary dominance. Genetics 172:713–718.

Turner, J. R. G. 1981. Adaptation and evolution in *Heliconius*: a defense of neoDarwinism. Annual Review of Ecology and Systematics 12:99–121.

Wang, J., and M. C. Whitlock. 2003. Estimating effective population size and migration rates from genetic samples over space and time. Genetics 163:429–446.

Waples, R. S. 2015. Testing for Hardy-Weinberg proportions: have we lost the plot? Journal of Heredity 106:1–19.

Willi, Y., M. Fracassetti, S. Zoller, and J. Van Buskirk. 2018. Accumulation of mutational load at the edges of a species range. Molecular Biology and Evolution 35:781–791.

Wright, S. 1931. Evolution in Mendelian populations. Genetics 16:97–159.

Zheng, Y., R. Peng, M. Kuro-o, and X. Zeng. 2011. Exploring patterns and extent of bias in estimating divergence time from mitochondrial DNA sequence data in a particular lineage: a case study of salamanders (order Caudata). Molecular Biology and Evolution 28:2521–2535.

Zimova, M., L. S. Mills, and J. J. Nowak. 2016. High fitness costs of climate change-induced camouflage mismatch. Ecology Letters 19:299–307.

Associate Editor: Katie E. Lotterhos
Editor: Daniel I. Bolnick